

On the First Law of Thermodynamics in Time-Dependent Open Quantum Systems

Parth Kumar* and Charles A. Stafford

Department of Physics, University of Arizona, 1118 East Fourth Street, Tucson, Arizona 85721, USA

(Dated: August 16, 2022)

How to rigorously define thermodynamic quantities such as heat, work, and internal energy in open quantum systems driven far from equilibrium remains a significant open question in quantum thermodynamics. Heat is a quantity whose fundamental definition applies only to processes in systems infinitesimally perturbed from equilibrium, and as such, must be accounted for carefully in strongly-driven systems. In this work, an unambiguous operator for the internal energy of an interacting time-dependent open quantum system is derived using a key insight from Mesoscopics: infinitely far from the local driving and coupling of an open quantum system, reservoirs are indeed only infinitesimally perturbed. Fully general expressions for the heat current and the power delivered by various agents to the system are derived using the formalism of nonequilibrium Green's functions, establishing an experimentally meaningful and quantum mechanically consistent division of the energy of the system under consideration into Heat flowing out of and Work done on the system. The spatio-temporal distribution of internal energy in a strongly-driven open quantum system is also analyzed. This formalism is applied to analyze the thermodynamic performance of a model quantum machine: a driven two-level quantum system strongly coupled to two metallic reservoirs, which can operate in several configurations—as a chemical pump/engine or a heat pump/engine.

CONTENTS

I. Introduction	1
II. The Time-Dependent Open Quantum System	2
A. Physical basis of the model Hamiltonian	3
III. Non-Equilibrium Thermodynamic Quantities	3
A. Work done by external forces	3
B. Particle Current	4
C. Heat Currents, Electrochemical Power, and the Role of Reservoirs	4
D. The First Law of Quantum Thermodynamics	4
E. Internal Energy Density	5
IV. Evaluating the Time-Dependent Energetics: NEGF Results	6
V. Proof of Concept: Application to a Driven Two-Level Quantum Machine	7
A. Machine Setup	7
B. Electrochemical Pump	7
C. Heat Engine	9
D. Spatio-Temporal Distribution of Internal Energy	10
VI. Conclusions	13
VII. Acknowledgments	14
References	14
A. Derivation of the NEGF formulas for all First Law quantities	16

B. Generalization to Time-Dependent reservoirs and coupling	18
---	----

I. INTRODUCTION

Quantum Thermodynamics has seen substantial progress in recent years in both experimental and theoretical directions. These include but are not limited to quantum thermometry [1–11], quantum and thermal machines [12–15], quantum stochastic dynamics [16–18] and quantum information and computation [19]. Despite these rapid advancements, however, broad consensus on several basic questions of the field has been elusive. The reason for this is not entirely mysterious. The field is, firstly in relative infancy and secondly a melding of two well-established disciplines of physics. A large subset of unresolved questions in quantum thermodynamics thus centers around the need for a careful evaluation of the foundational concepts and laws that the subject builds upon.

One of the key open questions has been the possibility and the formulation of the First Law of Thermodynamics for an open quantum system (defined as a quantum system statistically and quantum mechanically open to the environment via some coupling) driven far from equilibrium. More concretely, we may ask the following: how does one establish an experimentally meaningful and quantum mechanically consistent division of the energy of a far-from-equilibrium quantum system into its Internal Energy, the Work done by the different agents acting and boundary conditions imposed on it and the Heat flowing from it? An even more basic question that naturally precedes this is whether such a division is even possible given the fundamental uncertainty constraints that quantum mechanics places on the measurement of observables.

* parthk@arizona.edu

These questions have been previously addressed in several works [20–25], which present highly divergent points of view on the issue. Much of the controversy revolves around how to treat the “interface” between the system and the environment induced by the System-Reservoir coupling Hamiltonian. An approach based on the ‘Hamiltonian of Mean Force’ concept [20] introduces an ambiguity in the definition of Internal Energy of the system and concludes that it might not even be possible to formulate the First Law, even on a quantum-statistical average level. Another set of analyses [21, 22] proposes dividing up the Coupling energy between the system and the environment as half of it belonging to the system and half of it belonging to the environment. Others still, using the Master equation approach [23] and the so called Mesoscopic leads approach [24] conclude that the Internal energy of the nonequilibrium system should be identified by putting the entire Coupling with the System. A recent study comparing some of these approaches has also emerged [25].

In this work, we shed light on the problem of formulating the First Law of Thermodynamics for a time-dependent nonequilibrium quantum system using insights from Mesoscopic physics [26–29]. The mesoscopic modeling of the Hamiltonian governing the nonequilibrium dynamics is done such that the model is both experimentally realistic and computationally tractable while capturing all the relevant physics of the energy and particle flows. Specifically, we start by identifying the conditions under which heat can be unambiguously defined for a strongly-driven system and how one must account for it by carefully considering what role the Reservoirs (which make up the environment) coupled to the system play. This leads naturally to the identification that the Internal Energy operator should be the System Hamiltonian plus the full coupling Hamiltonian.

With the proper thermodynamic identifications made, we proceed to derive general expressions for all the different possible forms of energy flows out of the system using the nonequilibrium Green’s functions (NEGF) formalism. The NEGF formalism is a powerful framework for analyzing quantum transport which we utilize to investigate the thermodynamics of a fairly general structure, where the system consists of interacting electronic and phononic degrees of freedom which is strongly coupled to an environment of non-interacting electrons and phonons. As an application of these formal results, we simulate a strongly driven quantum machine based on Rabi oscillations of a double quantum dot system, investigating in detail its operation as an electrochemical pump and as a heat engine.

This work is organized as follows: In Section II, we give a detailed description of the model time-dependent Hamiltonian that forms the basis of all subsequent derivations and discussions. Section III identifies all the different possible forms of energy flow associated with the system, the role of reservoirs, and the consequent form of the Internal Energy Operator and the First Law. In Section

IV, we derive all the nonequilibrium energy flows in terms of the System Green’s functions using the NEGF formalism. In Section V, we present results and discussion for the simulation of the strongly-driven quantum machine operating as an electrochemical pump and a heat engine, including an analysis of the spatio-temporal distribution of the internal energy. Finally, the conclusions of our work are presented in Section VI.

II. THE TIME-DEPENDENT OPEN QUANTUM SYSTEM

A fairly general Hamiltonian for a time-dependent open quantum system can be written as

$$H(t) = H_S(t) + H_R + H_{SR}. \quad (1)$$

The System Hamiltonian $H_S(t)$ has explicit time-dependence due to an external drive and is written as the sum of electronic, phononic and electron-phonon coupling terms

$$H_S(t) = H_{S,el}(t) + H_{S,ph}(t) + H_{S,el-ph}. \quad (2)$$

The electronic part of the system Hamiltonian $H_{S,el}(t)$ includes electron-electron interactions and has explicit time-dependence from the external electric drive:

$$H_{S,el}(t) = \sum_{n,m} \left([H_{S,el}^{(1)}(t)]_{nm} d_n^\dagger d_m + [H_{S,el}^{(2)}]_{nm} d_n^\dagger d_m^\dagger d_m d_n \right), \quad (3)$$

where d_n^\dagger (d_n) creates (removes) an electron in the n^{th} orbital in the system and obeys fermionic anti-commutation $\{d_n^\dagger, d_m\} = \delta_{nm}$. The phononic part $H_{S,ph}(t)$ is given as the sum of a harmonic term and an anharmonic term

$$H_{S,ph}(t) = H_{S,ph}^{hm}(t) + H_{S,ph}^{ahm}, \quad (4)$$

where the time-dependent harmonic part $H_{S,ph}^{hm}(t)$ accounts for an external mechanical drive:

$$H_{S,ph}^{hm}(t) = \sum_{s,r} [H_{S,ph}^{(1)}(t)]_{sr} b_s^\dagger b_r \quad (5)$$

where b_r^\dagger (b_r) creates (removes) a phonon in the r^{th} mode in the system and obey the bosonic commutation $[b_r^\dagger, b_s] = \delta_{rs}$. The anharmonic part $H_{S,ph}^{ahm}$ is given by

$$H_{S,ph}^{ahm} = H_{S,ph}^{(3)} + H_{S,ph}^{(4)} + \dots, \quad (6)$$

where the cubic term $H_{S,ph}^{(3)}$ can be written as

$$H_{S,ph}^{(3)} = \sum_{n,m,o} [H_{S,ph}^{(3)}]_{nmo} q_n q_m q_o, \quad (7)$$

where the generalized coordinate q_n can be written in terms of normal coordinates as $q_n = \sum_r (Q_r e^{i r n} +$

$Q_r^\dagger e^{-irn}$) with $Q_r = \frac{1}{\sqrt{[H_{S,ph}^{(1)}(0)]_{rr}}}(b_r^\dagger + b_r)$. The quartic term $H_{S,ph}^{(4)}$ and all higher-order anharmonic terms can be written analogously. The electron-phonon coupling is

$$H_{S,el-ph} = \sum_{r,n,m} [H_{S,el-ph}]_{rnm} (b_r^\dagger + b_r) d_n^\dagger d_m + \dots \quad (8)$$

and may include higher-order terms in the lattice-electron potential expansion.

The environment is modeled as M perfectly ordered, semi-infinite Reservoirs of non-interacting electrons and phonons, each at Temperature T_α and chemical potential μ_α , with the Hamiltonian

$$H_R = \sum_{\alpha=1}^M \left(\sum_{k \in \alpha} \epsilon_k c_k^\dagger c_k + \sum_{q \in \alpha} \omega_q \left(a_q^\dagger a_q + \frac{1}{2} \right) \right). \quad (9)$$

where c_k^\dagger (c_k) creates (removes) an electron in eigenmode k in the reservoir and obey $\{c_k^\dagger, c_l\} = \delta_{kl}$, and a_q^\dagger (a_q) creates (removes) a phonon in the eigenmode q in the reservoir and obey $[a_q^\dagger, a_p] = \delta_{qp}$.

The coupling between the System and the Reservoirs is given by the Coupling Hamiltonian

$$H_{SR} = H_{SR,el} + H_{SR,ph}, \quad (10)$$

where

$$H_{SR,el} = \sum_{\alpha=1}^M \sum_{k \in \alpha, n} (V_{kn}^{el} c_k^\dagger d_n + h.c.) \quad (11)$$

and

$$H_{SR,ph} = \sum_{\alpha=1}^M \sum_{q \in \alpha, r} (V_{qr}^{ph} a_q^\dagger b_r + h.c.) \quad (12)$$

are the electronic and phononic parts of the coupling, respectively.

A. Physical basis of the model Hamiltonian

We note some points here about the modeling of the Hamiltonian just presented that are important from both physical and computational points of view.

First, the Reservoirs are modeled as non-interacting, semi-infinite, and perfectly ordered so that they faithfully represent the external macroscopic circuit used to impose any nonequilibrium bias on the system and to measure the resultant flows of charge and energy. As counters of charge and energy flowing out the system, it makes little sense to include two-body interactions in the Reservoirs, since that would significantly complicate the task of calculating these quantities, and many-body correlations are not relevant in such a macroscopic electric/thermal circuit in any case. The coupling between

the System and the Reservoir H_{SR} is also taken to be quadratic. Realistically, this is because the electrons in the metallic Reservoirs, modeled by H_R , are well screened and hence any interaction between the electrons in the System and the Reservoir can be treated with the method of image charges [30], the screening charges in the Reservoirs treated as slave degrees of freedom, rather than as independent quantum modes. This is justified because the screening charges in the reservoirs respond at the plasma frequency, which is much greater than typical response frequencies of a mesoscopic system.

Second, the number of Reservoir degrees of freedom entering H_{SR} is a set of measure zero [31, 32] compared to the full (infinite) Reservoir Hilbert space, with only a few frontier orbitals taking part in coupling the environment to the System. This is because tunnel coupling is local at the *Interface* between the System and Reservoir and the screening charges are also localized at the Interface [33]. The same holds true for the phononic degrees of freedom, whose elastic coupling is short-ranged [35]. A model calculation of the spatio-temporal dynamics of the Interface, illustrating these principles, is presented in Sec. VD.

III. NON-EQUILIBRIUM THERMODYNAMIC QUANTITIES

With the open quantum system defined, we now compute the nonequilibrium thermodynamic quantities of the system.

A. Work done by external forces

Following the so-called Inclusive definition of work, standard in the Quantum Thermodynamics literature [36] (in contrast with the Exclusive definition [37]), we identify the time rate of change of the expectation value of the total Hamiltonian as the rate of work done by external forces, $\dot{W}_{ext}(t)$, which for the form assumed for the Hamiltonian, we can compute as

$$\frac{d}{dt} \langle H(t) \rangle \equiv \dot{W}_{ext}(t) = \langle \dot{H}_S(t) \rangle. \quad (13)$$

The equality can be proved [38] by noting that $\langle H(t) \rangle = \mathbb{T}_R \{ \rho(t) H(t) \}$, with $\rho(t)$ denoting the full density matrix at time t and $\mathbb{T}_R \{ \}$ denoting the Trace operation, and using the chain rule we can write

$$\frac{d}{dt} \langle H(t) \rangle = \mathbb{T}_R \{ \dot{\rho}(t) H(t) + \rho(t) \dot{H}(t) \}, \quad (14)$$

which, with the equation of motion of the density matrix

$$i\hbar \dot{\rho} = [H(t), \rho(t)], \quad (15)$$

and cyclicity of the Trace gives the stated result, $\dot{W}_{ext}(t) = \langle \dot{H}_S(t) \rangle$, since the time-dependence is only in the System Hamiltonian $H_S(t)$.

Furthermore, since the time-dependence in $H_S(t)$ sits only in the one-body terms, we get

$$\dot{W}_{ext}(t) = \sum_{n,m,s,r} \langle [\dot{H}_{S,el}^{(1)}(t)]_{nm} d_n^\dagger d_m + [\dot{H}_{S,ph}^{(1)}(t)]_{sr} b_s^\dagger b_r \rangle. \quad (16)$$

B. Particle Current

The equation of motion for the expectation value of occupation number operator $N_\alpha = \sum_{k \in \alpha} c_k^\dagger c_k$ of reservoir α is

$$\frac{d}{dt} \langle N_\alpha \rangle = \frac{-i}{\hbar} \langle [N_\alpha, H(t)] \rangle = \frac{-i}{\hbar} \langle [N_\alpha, H_{SR}] \rangle, \quad (17)$$

which is just the electronic particle current $I_{\alpha,el}^N(t)$ for reservoir α . Using the identities $[A, BC] = \{A, B\}C - B\{C, A\} = [A, B]C - B[C, A]$, we obtain the particle current as

$$I_{\alpha,el}^N(t) = \frac{-i}{\hbar} \sum_{k \in \alpha, n} [V_{kn}^{el} \langle c_k^\dagger d_n \rangle - (V_{kn}^{el})^* \langle d_n^\dagger c_k \rangle]. \quad (18)$$

The electrical current is obtained by multiplying the above equation by the electric charge quantum.

C. Heat Currents, Electrochemical Power, and the Role of Reservoirs

We now compute the heat current by applying the fundamental thermodynamic identity at constant volume $dE = TdS + \mu dN$ to reservoir α

$$I_\alpha^Q(t) \equiv T_\alpha \frac{d}{dt} S_\alpha = \frac{d}{dt} \langle H_{R,\alpha} \rangle - \mu_\alpha \frac{d}{dt} \langle N_\alpha \rangle. \quad (19)$$

Carrying out commutator evaluations similar to that for the particle current, we get the electronic heat current [39]

$$I_{\alpha,el}^Q(t) = \frac{-i}{\hbar} \sum_{k \in \alpha, n} (\epsilon_k - \mu_\alpha) [V_{kn}^{el} \langle c_k^\dagger d_n \rangle - (V_{kn}^{el})^* \langle d_n^\dagger c_k \rangle], \quad (20)$$

which can be cast in terms of an energy weighted particle current (for the k^{th} mode) as

$$I_{\alpha,el}^Q(t) = \sum_{k \in \alpha, n} (\epsilon_k - \mu_\alpha) I_k^N(t), \quad (21)$$

where $I_k^N(t) = \frac{-i}{\hbar} [V_{kn}^{el} \langle c_k^\dagger d_n \rangle - (V_{kn}^{el})^* \langle d_n^\dagger c_k \rangle]$. The phononic heat current [40] can be analogously evaluated as

$$I_{\alpha,ph}^Q(t) = \frac{-i}{\hbar} \sum_{q \in \alpha, r} \omega_q [V_{qr}^{ph} \langle a_q^\dagger b_r \rangle - (V_{qr}^{ph})^* \langle b_r^\dagger a_q \rangle]. \quad (22)$$

Heat is a quantity whose fundamental definition $dQ = TdS$ is only valid for processes involving systems infinitesimally perturbed from equilibrium [41]. Furthermore, it represents an *irreversible flow* of energy, and as such, must be accounted for carefully in strongly-driven systems. These requirements are met exactly by the non-interacting semi-infinite reservoirs to which the nonequilibrium system is coupled. These properties of the reservoir model have been long established in the Mesoscopic and Quantum Transport literature [42–44], where they enforce an Ordering of Limits such that one must take the limit of the Reservoir size going to infinity $L \rightarrow \infty$ *before* taking limit of the adiabatic perturbation switch-on time going to infinity $t_{adiab} \rightarrow \infty$. Physically, t_{adiab} is related to the timescale of setting up and carrying out the experiment. This order of limits ensures that any electrons or phonons emitted by the System into the Reservoirs cannot be coherently backscattered into the system (causing decoherence of any quanta emitted into the Reservoirs despite the absence of 2-body interactions) and that the distributions of charge and energy in the Reservoirs cannot be depleted due to flows mediated by the System.

The time derivative of the expectation value of the Reservoir Hamiltonian has a simple interpretation: it is the total energy current flowing into the Reservoirs $\sum_\alpha I_\alpha^E(t)$ i.e.

$$\frac{d}{dt} \langle H_R(t) \rangle = \sum_\alpha I_\alpha^E(t). \quad (23)$$

At infinity, this in turn is just the electrical (or electrochemical) power delivered to the reservoir and the heat current flowing into it

$$\sum_\alpha I_\alpha^E(t) = \sum_\alpha \mu_\alpha I_{\alpha,el}^N(t) + \sum_\alpha I_\alpha^Q(t). \quad (24)$$

where $I_\alpha^Q(t) = I_{\alpha,el}^Q(t) + I_{\alpha,ph}^Q(t)$.

D. The First Law of Quantum Thermodynamics

From the discussion in III A, specifically Eq. (13), it follows that

$$\frac{d}{dt} \langle H_S(t) + H_{SR} + H_R \rangle = \dot{W}_{ext}(t). \quad (25)$$

Furthermore, with the identification of III C, specifically Eq. (24), we get

$$\frac{d}{dt} \langle H_S(t) + H_{SR} \rangle = \dot{W}_{ext}(t) + \left(\sum_\alpha -\mu_\alpha I_\alpha^N(t) \right) + \left(\sum_\alpha -I_\alpha^Q(t) \right). \quad (26)$$

It is then clear that the internal energy operator for the ‘‘System’’ must be recognized as sum of the System Hamiltonian and *full* Coupling Hamiltonian. Defining $\dot{W}_{elec}(t) := \sum_\alpha -\mu_\alpha I_{\alpha,el}^N(t)$ as the electrochemical power delivered to the system and $\dot{Q}(t) := \sum_\alpha -I_\alpha^Q(t)$ as the

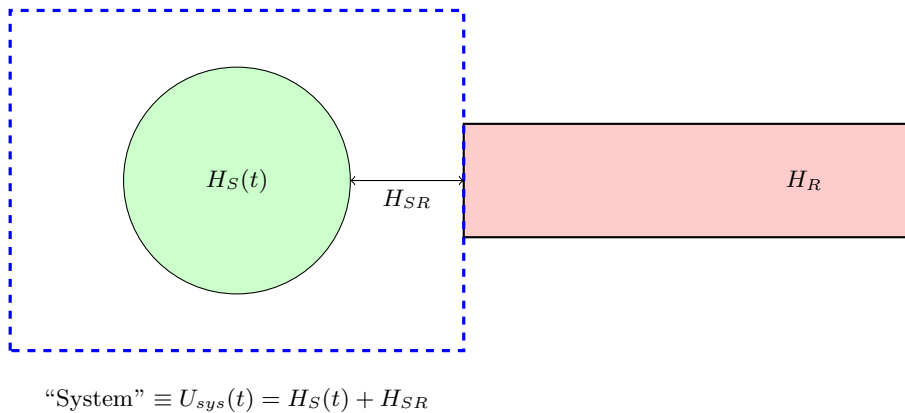


FIG. 1: Schematic representation of the energetic partitioning of a time-dependent open quantum system consistent with First Law of Quantum Thermodynamics [Eq. (27)]. This partitioning requires that the Internal Energy operator be identified as the sum of the System Hamiltonian $H_S(t)$ and the full coupling Hamiltonian H_{SR} describing the *Interface*; the spatial extent of this operator is denoted by the blue dashed box in the figure.

heat current flowing into the system allows us to write the First Law of Quantum Thermodynamics as

$$\frac{d}{dt}\langle U_{sys}(t) \rangle = \dot{W}_{ext}(t) + \dot{W}_{elec}(t) + \dot{Q}(t), \quad (27)$$

where we have the Internal Energy operator $U_{sys}(t)$ for the open quantum system

$$U_{sys}(t) = H_S(t) + H_{SR}. \quad (28)$$

This analysis lays to rest any ambiguity about the internal energy operator and gives a quantum mechanically consistent and experimentally meaningful division of the energetics of a fairly general open quantum system. Fig. 1 gives a schematic for this energy partitioning. We also note that this identification of the First Law and Internal Energy operator holds true in the even more general case where both the coupling and reservoirs become explicitly time-dependent, as discussed in Appendix B. The definition (28) agrees with that proposed by Strasberg and Winter [23] and Lacerda et al. [24], but disagrees with those put forward in Refs. [21, 22].

It should be noted, however, that as opposed to Internal Energy, Work being a path (and not a state) function cannot, in general, be a Quantum Operator [45, 46]. Furthermore, Heat (again a path function) also cannot have a quantum operator associated with it since it is a statistical quantity ($dQ = TdS$) defined unambiguously only under the special conditions discussed in III C.

E. Internal Energy Density

To further study the spatio-temporal distribution of the internal energy—for the special case where 2-body interactions are absent from the system—we make use of a general result for the spatial density of any one-body observable [47, 48].

The expectation value of the Internal energy operator $U_{sys}(t)$ identified in Eq. (28) is

$$\langle U_{sys}(t) \rangle = \text{Tr}\{\rho(t)U_{sys}(t)\}, \quad (29)$$

where $\rho(t)$ is the density matrix. If the position representation of the corresponding Hilbert space operator is $\langle x|u_{sys}(t)|y \rangle$ then the Fock space operator is

$$U_{sys}(t) = \int dx \int dy \hat{\psi}^\dagger(x) \langle x|u_{sys}(t)|y \rangle \hat{\psi}(y), \quad (30)$$

where $\hat{\psi}^\dagger(x)$ and $\hat{\psi}(y)$ are Fock space creation and annihilation operators in position representation, and the spin index has been suppressed for simplicity.

We define the Fock space internal energy density operator as

$$\varrho_{u_{sys}}(x, t) = \frac{1}{2} \int dy \hat{\psi}^\dagger(x) \langle x|u_{sys}(t)|y \rangle \hat{\psi}(y) + \frac{1}{2} \int dy \hat{\psi}^\dagger(y) \langle y|u_{sys}(t)|x \rangle \hat{\psi}(x), \quad (31)$$

which evidently satisfies the condition

$$U_{sys}(t) = \int dx \varrho_{U_{sys}}(x, t). \quad (32)$$

The internal energy density is

$$\rho_{U_{sys}}(x, t) = \text{Tr}\{\rho(t)\varrho_{U_{sys}}(x, t)\}, \quad (33)$$

and from Eq. (28) it follows directly that

$$\rho_{U_{sys}}(x, t) = \rho_{H_S}(x, t) + \rho_{H_{SR}}(x, t), \quad (34)$$

where $\rho_{H_S}(x, t)$ and $\rho_{H_{SR}}(x, t)$ are defined analogously to $\rho_{U_{sys}}(x, t)$, using the one-body Hilbert-space operators corresponding to $H_S(t)$ and H_{SR} , respectively.

IV. EVALUATING THE TIME-DEPENDENT ENERGETICS: NEGF RESULTS

We employ the Nonequilibrium Green's function (NEGF) formalism [26, 27, 49–51] to evaluate all the terms appearing in the First Law (27), each term on the LHS of which we have evaluated in terms of the expectation values in Eqs. (16), (18), (21) and (22). Here we present only the final results of our analysis and defer the relevant details of the derivations and methods of evaluation to Appendix A. We also note that the NEGF formalism has a well-established connection with the S-Matrix formalism [52]—another technique often employed in quantum transport and thermodynamics. A key advantage of NEGF is its simplicity and power in computing one-body (or even few-body) observables. This is in contrast to the Master equation approach [26, 28, 53], which works in the full many-particle Hilbert space.

The electronic particle current, given by the Jauho-Wingreen-Meir formula [54, 55], is

$$I_{\alpha,el}^N(t) = \frac{2}{\hbar} \int_{-\infty}^{\infty} \frac{dE}{2\pi} \int_{-\infty}^t dt_1 \text{Im} \text{Tr} \{ e^{-iE(t_1-t)} \Gamma_{\alpha}^{el}(E) [G^{<,el}(t, t_1) + f_{\alpha}(E) G^{R,el}(t, t_1)] \}, \quad (35)$$

where $\Gamma_{\alpha}^{el}(E)$, $G^{<,el}(t, t')$ and $G^{R,el}(t, t')$ are understood to be matrices. The system electronic Lesser and Retarded Green's functions are defined as (see Appendix A for the method of their evaluation)

$$G_{nm}^{<,el}(t, t_1) = i \langle d_m^{\dagger}(t_1) d_n(t) \rangle \quad (36)$$

and

$$G_{nm}^{R,el}(t, t_1) = -i \theta(t - t_1) \langle \{ d_n(t), d_m^{\dagger}(t_1) \} \rangle, \quad (37)$$

respectively, where $\langle \rangle$ denotes the quantum and statistical average, and

$$f_{\alpha}(\epsilon_k) = \frac{1}{e^{\beta_{\alpha}(\epsilon_k - \mu)} + 1} \quad (38)$$

is the Fermi-Dirac distribution function of reservoir α with $\beta_{\alpha} = (k_B T_{\alpha})^{-1}$, where k_B is the Boltzmann Constant. Following [56], we identify the electronic tunneling-width matrix $\Gamma_{\alpha}^{el}(E)$ as

$$[\Gamma_{\alpha}^{el}(E)]_{nm} = \sum_{k \in \alpha} 2\pi \delta(E - \epsilon_k) V_n^{el}(E) (V_m^{el})^*(E), \quad (39)$$

with $V_n^{el}(E) = V_{kn}^{el}$ when $E = \epsilon_k$. The electronic heat current formula (20) becomes (see Appendix A for a derivation)

$$I_{\alpha,el}^Q(t) = \frac{2}{\hbar} \int_{-\infty}^{\infty} \frac{dE}{2\pi} \int_{-\infty}^t dt_1 (E - \mu_{\alpha}) \text{Im} \text{Tr} \{ e^{-iE(t_1-t)} \Gamma_{\alpha}^{el}(E) [G^{<,el}(t, t_1) + f_{\alpha}(E) G^{R,el}(t, t_1)] \}, \quad (40)$$

which generalizes the Bergfield-Stafford formula [39] to the case of a time-dependent system. The electronic (heat and particle) currents flowing into reservoir α can be cast in a compact form

$$I_{\alpha,el}^{(\nu)}(t) = \frac{2}{\hbar} \int_{-\infty}^{\infty} \frac{dE}{2\pi} (E - \mu_{\alpha})^{\nu} \int_{-\infty}^t dt_1 \text{Im} \text{Tr} \{ e^{-iE(t_1-t)} \Gamma_{\alpha}^{el}(E) [G^{<,el}(t, t_1) + f_{\alpha}(E) G^{R,el}(t, t_1)] \}, \quad (41)$$

where ($\nu = 0$) gives the electronic particle current and ($\nu = 1$) gives the electronic heat current.

The phononic heat current is obtained similarly in terms of the system Phononic Green's functions as

$$I_{\alpha,ph}^Q(t) = \frac{2}{\hbar} \int_{-\infty}^{\infty} \frac{dE}{2\pi} E \int_{-\infty}^t dt_1 \text{Im} \text{Tr} \{ e^{-iE(t_1-t)} \Gamma_{\alpha}^{ph}(E) [G^{<,ph}(t, t_1) + f_{\alpha}^{Planck}(E) G^{R,ph}(t, t_1)] \}, \quad (42)$$

where we have the system phononic Green's functions

$$G_{rs}^{<,ph}(t, t_1) = i \langle b_s^{\dagger}(t_1) b_r(t) \rangle \quad (43)$$

and

$$G_{rs}^{R,ph}(t, t_1) = -i \theta(t - t_1) \langle [b_r(t), b_s^{\dagger}(t_1)] \rangle, \quad (44)$$

and the phononic tunneling-width matrix

$$[\Gamma_{\alpha}^{ph}(E)]_{rs} = \sum_{q \in \alpha} 2\pi \delta(\omega - \omega_q) V_r^{ph}(E) (V_s^{ph})^*(E), \quad (45)$$

and

$$f_{\alpha}^{Planck}(\epsilon_q) = \frac{1}{e^{\beta_{\alpha}(\epsilon_q)} - 1} \quad (46)$$

is the Planck distribution function of reservoir α .

Finally, the work done by external forces can also be written in terms of the system Green's functions as

$$\dot{W}_{ext} = -i \text{Tr} \{ \dot{H}_{S,el}^{(1)}(t) G^{<,el}(t, t) + \dot{H}_{S,ph}^{(1)}(t) G^{<,ph}(t, t) \}. \quad (47)$$

The expectation value of the internal energy operator defined in Eq. (28) can also be evaluated in terms of the system Green's functions. The first term is

$$\begin{aligned} \langle H_S(t) \rangle = & -i \text{Tr} \{ H_{S,el}^{(1)}(t) G^{<,el}(t, t) + H_{S,ph}^{(1)}(t) G^{<,ph}(t, t) \\ & + H_{S,el}^{(2)} G^{(2),el}(t, t) + H_{S,ph}^{(3)} G^{(3),ph}(t, t) \\ & + H_{S,el-ph}^{(2)} G^{(2),el-ph}(t, t) \}, \end{aligned} \quad (48)$$

where the 2-body and higher electronic and phononic Green's functions are defined as $G_{nnmm}^{(2),el}(t, t) = i \langle d_n^{\dagger}(t) d_m^{\dagger}(t) d_m(t) d_n(t) \rangle$, $G_{rnm}^{(2),el-ph}(t, t) = i \langle [b_r^{\dagger}(t) + b_r(t)] d_n^{\dagger}(t) d_m(t) \rangle$, and $G_{nm\phi}^{(3),ph}(t, t) = i \langle q_n(t) q_m(t) q_{\phi}(t) \rangle$, respectively (higher order phononic Green's functions can

be constructed analogously). The second term in the internal energy may be evaluated as (see Appendix A for details)

$$\langle H_{SR}(t) \rangle = \frac{2}{\hbar} \int_{-\infty}^{\infty} \frac{dE}{2\pi} \int_{-\infty}^t dt_1 \text{ReTr} \{ e^{-iE(t_1-t)} (\Gamma_{\alpha}^{el}(E)[G^{<,el}(t, t_1) + f_{\alpha}(E)G^{R,el}(t, t_1)] + \Gamma_{\alpha}^{ph}(E)[G^{<,ph}(t, t_1) + f_{\alpha}^{Planch}(E)G^{R,ph}(t, t_1)]) \}. \quad (49)$$

With this, all the terms appearing in the First Law [Eq. (27)] have now been evaluated in terms of system Green's functions, and we identify $I_{\alpha,el}^N(t) = I_{\alpha,el}^{(0)}(t)$ and $I_{\alpha}^Q(t) = I_{\alpha,el}^{(1)}(t) + I_{\alpha,ph}^Q(t)$, so that $\dot{W}_{elec}(t)$ and $\dot{Q}(t)$ are defined exactly as in Sec. III D.

Finally, both terms on the RHS of Eq. (34) for the internal energy density can also be evaluated in terms of the Green's functions in a similar manner, giving

$$\rho_{HS}(x, t) = \text{Im}[\langle x | h_{S,el}^{(1)}(t) G^{<,el}(t, t) + h_{S,ph}^{(1)}(t) G^{<,ph}(t, t) | x \rangle], \quad (50)$$

and

$$\rho_{HSR}(x, t) = \text{Im}[\langle x | h_{SR,el} G_{tun}^{<,el}(t, t) + h_{SR,ph} G_{tun}^{<,ph}(t, t) | x \rangle], \quad (51)$$

where $h_{S,el/ph}^{(1)}$ are Hilbert-space operators corresponding to the one-body part of the Fock-space system Hamiltonians defined in Eqs. (3) and (5) and $h_{SR,el/ph}$ are Hilbert-space operators corresponding to the Fock-space coupling Hamiltonians defined in Eqs. (11) and (12), while $G_{tun,kn}^{<,el}(t, t) = i \langle d_n^{\dagger}(t) c_k(t) \rangle$ and $G_{tun,qr}^{<,ph}(t, t) = i \langle b_r^{\dagger}(t) a_q(t) \rangle$ are the tunneling Green's functions for the electrons and phonons respectively.

V. PROOF OF CONCEPT: APPLICATION TO A DRIVEN TWO-LEVEL QUANTUM MACHINE

We have applied our formal results to perform a complete thermodynamic analysis of a strongly driven two-level quantum system coupled to two metallic reservoirs. We first describe the basic setup of the quantum machine, followed by a detailed analysis of its operation in two different configurations. This simulation underscores the utility of our formal results derived in the previous sections, as tools to investigate the real-time dynamics of quantum systems driven far from equilibrium.

A. Machine Setup

The quantum machine consists of two (spatially separated) quantum dots, each with a single active level, with energies E_1 and E_2 , coupled to each other via inter-dot coupling w . The system is opened to the environment by coupling each dot to a perfectly ordered,

semi-infinite Fermionic reservoir via energy-independent tunneling-width matrix elements $\Gamma_1 = \Gamma_2 = \Gamma$. Both reservoirs are maintained in internal equilibrium characterized by fixed Chemical Potentials and Temperatures μ_1, T_1 and μ_2, T_2 (see Ref. [57] for an analysis of a similar quantum machine). The time-dependent drive is applied only to one of the dots (the dot with energy E_1 for the results presented) and is set up as a rectangular pulse of strength δ which is active for a duration τ . The pulse strength δ is set equal to the difference between the dot energies $\Delta E = E_2 - E_1$ and brings the two levels into resonance, allowing the electron density to strongly Rabi oscillate between them. The pulse duration is tuned as a π -pulse by setting $\tau = \frac{\pi}{2w}$. This maximizes the probability of transferring the electron density from one dot to the other at the end of the pulse. We also order the parameters such that $\Delta E \gg w \gg \Gamma$ to ensure that the levels remain highly localized in the absence of a drive.

The energy parameters of the system can be tuned relative to each other such that its Rabi Oscillations can be leveraged to operate it as an Electrochemical Pump, an Electrochemical Engine, a Heat Engine, and a Heat Pump. Here we present a detailed analysis for the Electrochemical Pump and Heat Engine configurations.

B. Electrochemical Pump

For the setup described, if the electrochemical potentials of the reservoirs are biased such that $\mu_1 > E_1$ and $\mu_2 < E_2$, electrons can be pumped uphill from the left to the right reservoir. A schematic of the chemical pump configuration is shown in Fig. 2. In this configuration, the Temperatures T_1, T_2 of the reservoirs are set to very low values to suppress any thermal excitations from contributing to the operation. The thermodynamic cycle for the pump involves the electron tunneling from the left reservoir to dot 1 followed by the pulse raising its energy to bring it into resonance with dot 2. The π -pulse ensures a maximum probability of dot 2 capturing the electron at the end of the pulse which is followed by the electron tunneling out into the right reservoir. The machine relaxes back to its initial state at late times, at which point we can calculate the efficiency of the electrochemical pump as

$$\eta_{EP} = \frac{|W_{elec}(\infty)|}{|W_{ext}(\infty)|}. \quad (52)$$

The full Hamiltonian for this configuration is given by Eq. (1), where the System Hamiltonian is given specifically by

$$H_S(t) = E_1(t) d_1^{\dagger} d_1 + E_2 d_2^{\dagger} d_2 + w(d_1^{\dagger} d_2 + d_2^{\dagger} d_1), \quad (53)$$

with the Reservoir Hamiltonian given by

$$H_R = \sum_{i=1,2} \sum_{k \in i} \epsilon_k c_k^{\dagger} c_k, \quad (54)$$

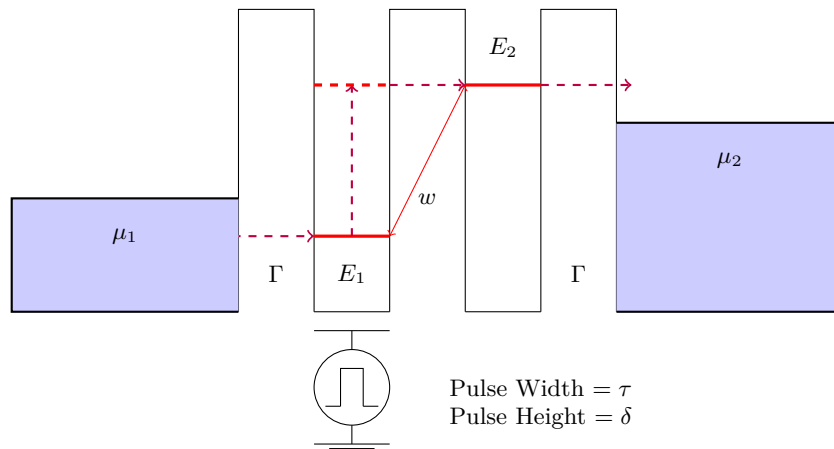


FIG. 2: Schematic representation of an Electrochemical Pump based on Rabi Oscillations between states of a double quantum dot. The left and right dots in the system have on-site energies E_1 and E_2 , respectively, and are coupled by a constant hopping matrix element w . The left dot is driven by a rectangular pulse of width τ and height δ . Each dot is coupled with the same Tunneling width matrix element Γ to a Reservoir. The Reservoirs are modeled as non-interacting, Fermionic, semi-infinite reservoirs at Electrochemical Potentials μ_1 and μ_2 for the left and right reservoirs, respectively, with $T_2 = T_1$. The cycle of operation of the electrochemical pump is denoted by the dashed purple arrows.

and the coupling is such that the i^{th} dot is only coupled to the i^{th} reservoir

$$H_{SR} = \sum_{k \in 1} (V_{k1} c_k^\dagger d_1 + h.c.) + \sum_{k \in 2} (V_{k2} c_k^\dagger d_2 + h.c.). \quad (55)$$

Finally, the time dependence of the system is encoded in the left dot as

$$E_1(t) = \begin{cases} E_1 & t < 0, \\ E_1 + \delta & 0 < t < \tau, \\ E_1 & t > \tau. \end{cases} \quad (56)$$

Fig. 3 shows plots of all the thermodynamic quantities entering the First Law as functions of time. We note that we have plotted the integrated thermodynamic quantities here instead of the time-derivatives that appear in our First Law equation [Eq. (27)], so that we have the total external work done on the system $W_{ext}(t) = -i \int_{-\infty}^t dt \text{Tr} \{ \dot{H}_S^{(1)}(t) G^<(t, t) \}$, the total electrical work done on the system $W_{elec}(t) = \int_{-\infty}^t dt [\sum_{\alpha} -\mu_{\alpha} I_{\alpha}^{(0)}(t)]$, and the total heat dissipated into the reservoirs $-Q(t) = \int_{-\infty}^t dt (\sum_{\alpha} I_{\alpha}^{(1)}(t))$. All the energies reported for this setup are in units of the on-site energy of the right dot E_2 and time is in units of E_2^{-1} .

The total external work done by the drive $W_{ext}(t)$, (Fig. 3a) follows the expected instantaneous rise of the pulse at $t = 0$ to a value of 1.87, indicating that work is done *on* the system by the drive. $W_{ext}(t)$ remains at this constant value for the duration of the pulse τ , followed by a slight instantaneous decrease at $t = \tau$. This can be explained by noting that there is a small but finite probability for the electron being on dot 1 at the end of the π -pulse. This results in work being done *by* the system

on the drive as the energy of the first dot is lowered back to its initial value, appearing as a negative contribution. The external work done remains constant at a value of 1.78 thereafter since the drive is inactive for $t > \tau$.

As the pulse starts, the electrical work $W_{elec}(t)$, (Fig. 3b) is done *on* the system as the particle current flows mostly into the left reservoir initially. At a certain time $t > \tau$ the electrochemical work becomes negative indicating that chemical work is now done *by* the system as the particle current starts to flow mostly into the right reservoir. It increases in magnitude for some time and eventually attains a constant value of -0.65 at late times as the particle currents flowing into the reservoirs relax to 0. For the complete cycle, electrical work is thus done by the system in transferring an electron from the reservoir with the lower chemical potential μ_1 to the one with the higher chemical potential μ_2 . With the late time values of $W_{elec}(t)$ and $W_{ext}(t)$, we can see that the efficiency of the electrochemical pump η_{EP} is about 36.5%.

The total heat dissipated into the reservoirs $-Q(t)$ (Fig. 3c) always remains positive implying that heat is only ever flowing into the reservoirs in the electrochemical pump configuration for the parameters chosen. This can be explained by noting that the (steady-state) heat flowing into the i^{th} reservoir goes as $(E_i - \mu_i) v_i f_i(E)$, where v_i is the velocity of the electron [58]. The levels in the numerics are biased such that $(E_i - \mu_i) v_i$ always remains positive for both reservoirs, no matter which direction the electron is moving. The pronounced knee at $t = \tau$ is due to the opening up of another transport channel at the first dot in the form of a hole channel once the electron has been captured by the second dot at the end of the pulse and the left dot is in an empty state. The total heat dissipated asymptotes to a constant value of

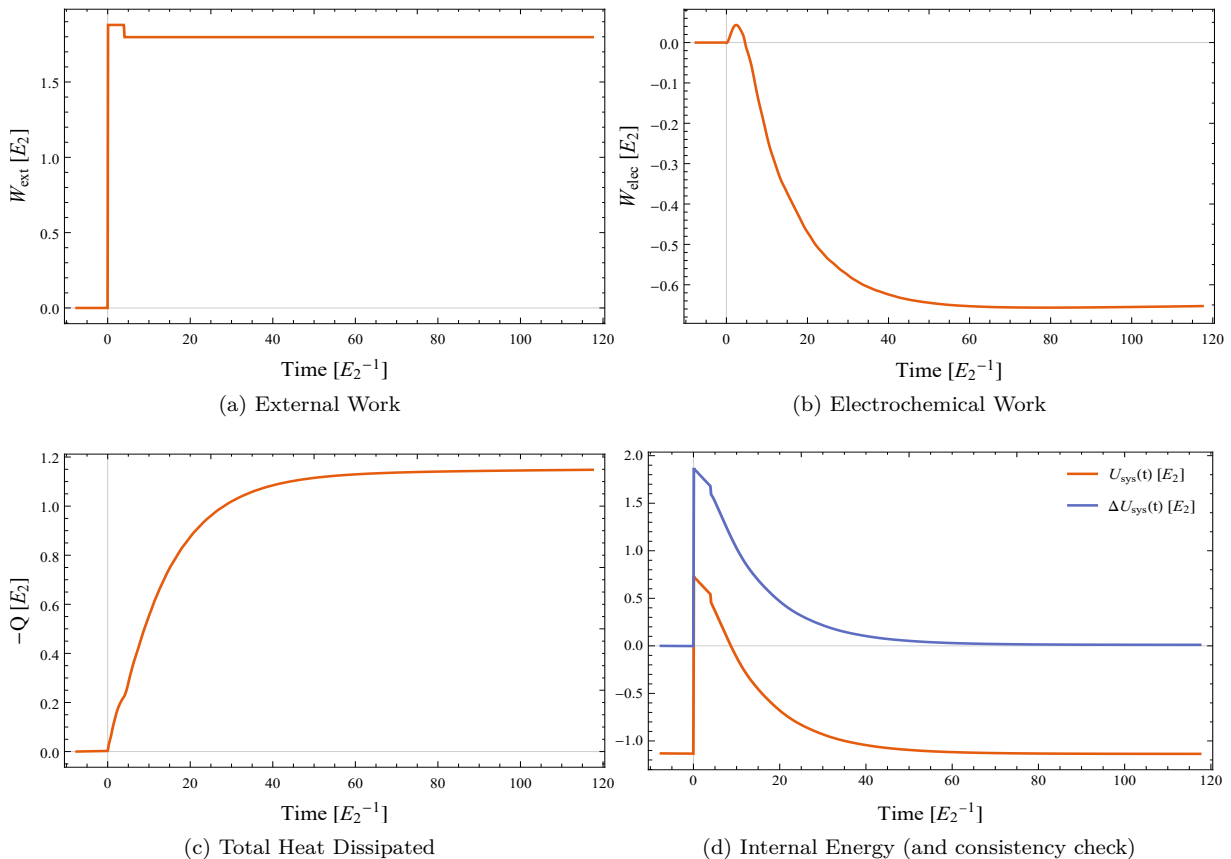


FIG. 3: The time-dependent energetics of the Electrochemical Pump depicted schematically in Fig. 2. (a) Total work done by external drive versus time, (b) Total electrochemical work done versus time, (c) Total Heat dissipated into reservoirs versus time, (d) Internal Energy U_{sys} (in orange) and ΔU_{sys} from integration of the RHS of the First Law equation (27) (in blue) versus time. For the results shown we have used $\hbar = 1$ and we set the on-site energy on the left and right dots $\{E_1, E_2\} = \{-1, 1\}$ so that the difference in the on-site energies of the two dots is $\Delta E = E_2 - E_1 = 2$ in units of E_2 . The dot hybridization is set to $w = \Delta E/5$ and the coupling to the reservoirs is taken as $\Gamma = w/5$. The chemical potential and temperatures of the reservoirs are set $-\mu_1 = \mu_2 = 0.5$ in units of E_2 and $k_B T_1 = k_B T_2 = 0.016$ in units of E_2 , respectively. The pulse amplitude is set equal to the difference in the on-site energies $\delta = \Delta E$ and the pulse duration is set $\tau = \pi/2w$ (π -pulse).

1.17 at late times.

We finally plot the internal energy $U_{\text{sys}}(t)$ (Fig. 3d) and note that it matches up well with the plot of the sum of all the terms appearing on the right hand side of the First Law i.e., $\Delta U_{\text{sys}}(t) = W_{\text{ext}}(t) + W_{\text{elec}}(t) + Q(t)$. The offset is expected since we have plotted $U_{\text{sys}}(t)$ directly from the Eqs. (48) and (49), which are expressions for energy, whereas the plot of $\Delta U_{\text{sys}}(t)$ was generated by integration of the current formulas where the constant of integration was set to 0.

C. Heat Engine

For the heat engine configuration, the temperatures are raised to significant unequal values ($T_2 > T_1$) comparable to that of the system energy levels, and the chemical

potentials of both the reservoirs are set to zero, $\mu_1 = \mu_2 = 0$. Furthermore, in addition to the left dot energy, the inter-dot coupling is now a function of time $w \rightarrow w(t)$. Specifically, it is activated to a constant value w only during the pulse and is zero before and after it. This is done to suppress heat flow into the reservoirs before and after the pulse thus increasing the efficiency of the heat engine

$$\eta_{HE} = \frac{|W_{\text{ext}}(\infty)|}{|Q_2(\infty)|}, \quad (57)$$

where $Q_2(\infty)$ is the heat extracted from the right reservoir at late times.

Again, the full Hamiltonian for this configuration is given by Eq. (1) and the System Hamiltonian is given specifically by

$$H_S(t) = E_1(t)d_1^\dagger d_1 + E_2 d_2^\dagger d_2 + w(t)(d_1^\dagger d_2 + d_2^\dagger d_1), \quad (58)$$

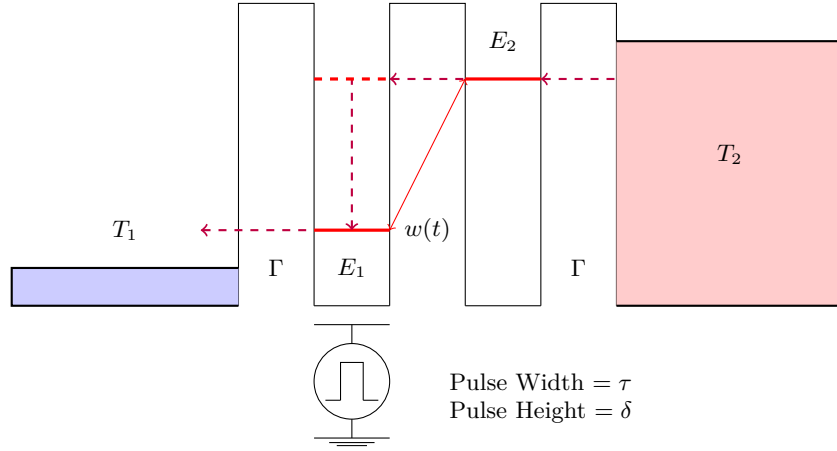


FIG. 4: Schematic representation of a Heat Engine based on Rabi Oscillations between states of a double quantum dot. The left and right dots in the system have on-site energies E_1 and E_2 , respectively, and are dynamically coupled by a time-dependent hopping term $w(t)$. The left dot is driven by a rectangular pulse of width τ and strength δ . Each dot is coupled with the same Tunneling width matrix element Γ to a Reservoir. The Reservoirs are modeled as non-interacting, Fermionic, semi-infinite systems at Temperatures T_1 and T_2 for the left and right reservoirs, respectively, with $T_2 > T_1$. The cycle of operation of the heat engine is denoted by the dashed purple arrows.

with the Reservoir and Coupling Hamiltonian exactly the same as in the electrochemical pump case given by Eqs. (54) and (55), respectively.

As before, the rectangular pulse acts only on the left dot with $E_1(t)$ given by Eq. (56), and the time-dependent inter-dot coupling is

$$w(t) = \begin{cases} 0 & t < 0, \\ w & 0 < t < \tau, \\ 0 & t > \tau. \end{cases} \quad (59)$$

In the heat engine configuration, the electron transport path is essentially reversed from the pump configuration. The electron tunnels in from the right reservoir on to the right dot, Rabi Oscillates onto the left dot, is lowered to energy E_1 at the end of the pulse and tunnels out into the left reservoir, accomplishing engine operation. A schematic for the engine is given in Fig. 4.

The time-dependent energetics shown in Fig. 5, where all the energies are reported in units of the on-site energy of the left dot E_1 and time is in units of E_1^{-1} , demonstrate that external work $W_{ext}(t)$ (Fig. 5a) is now done by the engine on the drive as the left dot is lowered at the end of the pulse. For the parameters chosen $W_{ext}(t)$ at late times attains a constant value of -0.18 . This work is done by extracting heat $Q_2(t)$ (Fig. 5b) from the hot reservoir at T_2 , and eventually attains a constant value of -0.60 at late times after the pulse and inter-dot coupling are inactivated.

By design, no net electrochemical is work done (Fig. 5c) since we had set the chemical potentials of both the reservoirs to 0 in this configuration. Finally, the left and right hand sides of the First Law are again in good agreement (Fig. 5d), up to a constant of integration offset. For

the parameters chosen, the heat engine operates at an efficiency η_{HE} of about 46.5% which is close to 53% of Carnot efficiency.

D. Spatio-Temporal Distribution of Internal Energy

To investigate the spatio-temporal distribution of energy in the driven quantum machine, we utilize the theory of internal energy density developed in Sec. III E. We work with essentially the same setup as in the previous two subsections, but now with a specific model for the reservoirs: 1D tight-binding chains. The System Hamiltonian $H_S(t)$ is chosen the same as in the electrochemical pump case [Eq. (53)]. The Reservoir Hamiltonian is

$$H_R = \sum_{\alpha=L,R} \left[\sum_{j=1}^{\infty} \epsilon_0 c_{j\alpha}^\dagger c_{j\alpha} + \sum_{j=1}^{\infty} t_0 (c_{j\alpha}^\dagger c_{j+1\alpha} + h.c.) \right], \quad (60)$$

where ϵ_0 is the on-site energy at any given site and t_0 is the hopping integral between nearest-neighbor sites on a given chain. The Coupling Hamiltonian is

$$H_{SR} = t \left[(d_1^\dagger c_{1L} + h.c.) + (d_2^\dagger c_{1R} + h.c.) \right], \quad (61)$$

where t is the coupling between the first site in the left reservoir $1L$ and the left dot, and that between the first site in the right reservoir $1R$ and the right dot. A schematic of this setup is given in Fig. 6 (Right Panel).

We study the internal energy density $\rho_{U_{sys}}$ of the system, given by Eq. (34), as a function of time. Due to

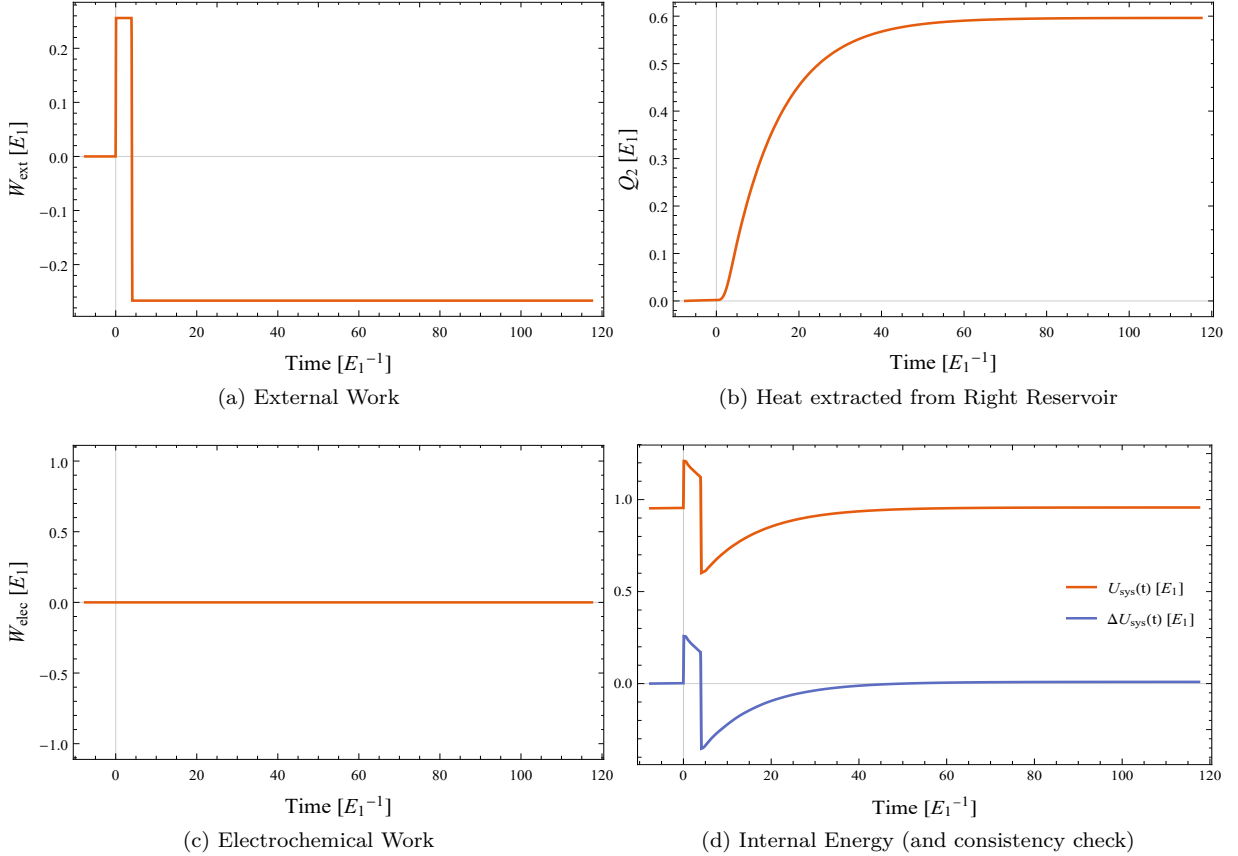


FIG. 5: The Time-dependent energetics of the Heat Engine depicted schematically in Fig. 4. (a) Total work done by external drive versus time, (b) Heat extracted from the right (hot) Reservoir, (c) Total electrochemical work done versus time, (d) Internal Energy (in orange) and RHS of the First Law equation (27) (in blue) versus time. For the results shown, we have used $\hbar = 1$ and we set the on-site energy on the left and right dots to $\{E_1, E_2\} = \{1, 3\}$ so that the difference in the on-site energies of the two dots is $\Delta E = E_2 - E_1 = 2$ in units of E_1 . The dot hybridization (when non-zero during the pulse) is set $w = \Delta E/5$ and the coupling to the reservoirs is taken as $\Gamma = w/5$. The chemical potentials and temperatures of the reservoirs are set to $\mu_1 = \mu_2 = 0$ and $\{k_B T_1, k_B T_2\} = \{0.5, 3.6\}$ in units of E_1 , respectively. The pulse amplitude is set equal to the difference in the on-site energies $\delta = \Delta E$ and the pulse duration is set $\tau = \pi/2w$ (π -pulse).

the short-range coupling between the system and reservoirs, $\rho_{U_{sys}}$ extends spatially only to the first site on the left reservoir chain ($1L$), the left dot ($D1$), the right dot ($D2$), and the first site on the right reservoir chain ($1R$). All other sites have zero contribution from the internal energy operator for this model. The tunneling-width matrices for the 1D tight-binding chains coupled to the double quantum dot system are [59, 60]

$$[\Gamma_\alpha(E)]_{ij} = \begin{cases} \frac{2t^2}{t_0} \left(1 - \left(\frac{\epsilon_0 - E}{2t_0}\right)^2\right)^{\frac{1}{2}} \delta_{i\alpha} \delta_{j\alpha}, & |E - \epsilon_0| < 2t_0, \\ 0, & \text{otherwise.} \end{cases} \quad (62)$$

The numerical results for the internal energy density are shown in the left panel of Fig. 6 for the system in the electrochemical pump configuration (Sec. VB) [61]. The internal energy on the left dot $\rho_{U_{sys}}(D1, t)$ (Fig. 6b) rises instantaneously to its maximum positive value at

the start of the pulse as the external drive does work *on* the dot. As the electron Rabi oscillates onto the right dot, the energy on the left dot begins to decrease and at the end of the pulse becomes zero and then asymptotes to its initial value as the initial conditions of the system are established again at late times. The Rabi oscillations of the system become more evident for the case of a 3π -pulse, as seen in Fig. 7, where we have again plotted the internal energy density $\rho_{U_{sys}}(x, t)$ [Eq. (34)] for both the dots and first sites of both reservoirs.

The energy at the first site in the left reservoir $\rho_{U_{sys}}(1L, t)$ (Fig. 6a) rises and falls in response to changes in the energy on Dot 1. This “in-phase with $D1$ ” behavior can be understood by noting first that $\rho_{H_S}(1L, t) = 0$ so that $\rho_{U_{sys}}(1L, t) = \rho_{H_{SR}}(1L, t)$. H_{SR} models the covalent bond between the dot and the first site on the chain which is equally shared between the two. Negative (posi-

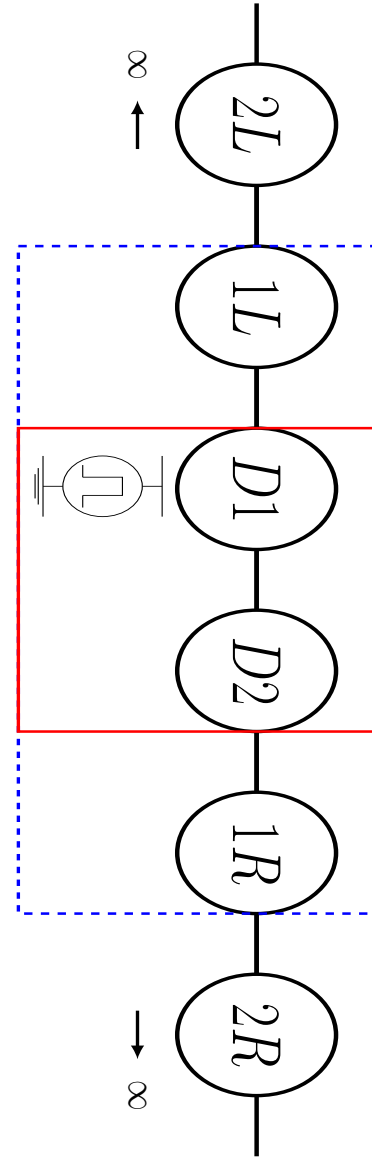
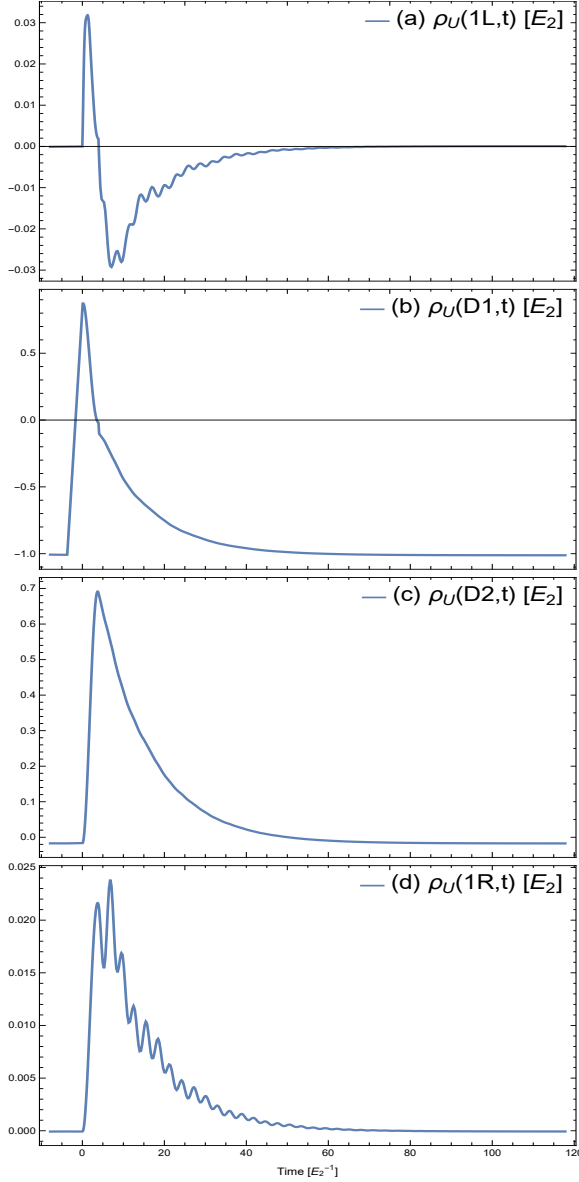


FIG. 6: *Left Panel:* Plots of Internal Energy as a function of time for the same double quantum dot system as in Sec. VB, now coupled specifically to semi-infinite tight-binding chains. The left and right dots are labeled as D1 and D2, respectively, and the chain sites on the left and right reservoirs are labelled as 1L, 2L,... and 1R, 2R,..., respectively. Only the site 1L is directly coupled to D1 and only the site 1R is directly coupled to D2. The Internal Energy is denoted by $\rho_U(1L, t)$ on the first site on the left chain, by $\rho_U(D1, t)$ on the left dot, by $\rho_U(D2, t)$ on the right dot, and by $\rho_U(1R, t)$ on the first site on the right chain. Note that the energy scale for $\rho_U(1L, t)$ and $\rho_U(1R, t)$ is different from that for $\rho_U(D1, t)$ and $\rho_U(D2, t)$ in the figure. *Right Panel:* Schematic representation of the system. The solid red box denotes the spatial extent of the degrees of freedom of the System Hamiltonian $H_S(t)$ and the dashed blue box denotes the spatial extent of the Internal Energy operator $U_{sys}(t) = H_S(t) + H_{SR}$. The energies are in units of the on-site energy of the right dot E_2 and time is in units of E_2^{-1} .

tive) bond energies correspond to bonding (anti-bonding) character of the Dot-Reservoir interface. The bond energy tends to zero at long times as the system relaxes to its initial state wherein the occupancy of Dot 1 is nearly unity so that the hybridization with the left Reservoir tends to zero. The oscillatory behavior during the relax-

ation is a signature of the Rabi oscillations between the two dots D1 and D2, which are enhanced in frequency (but suppressed in amplitude) when the pulse is inactivated.

The energy on the right dot $\rho_{U_{sys}}(D2, t)$ (Fig. 6c) rises as the electron Rabi oscillates onto it from the left dot

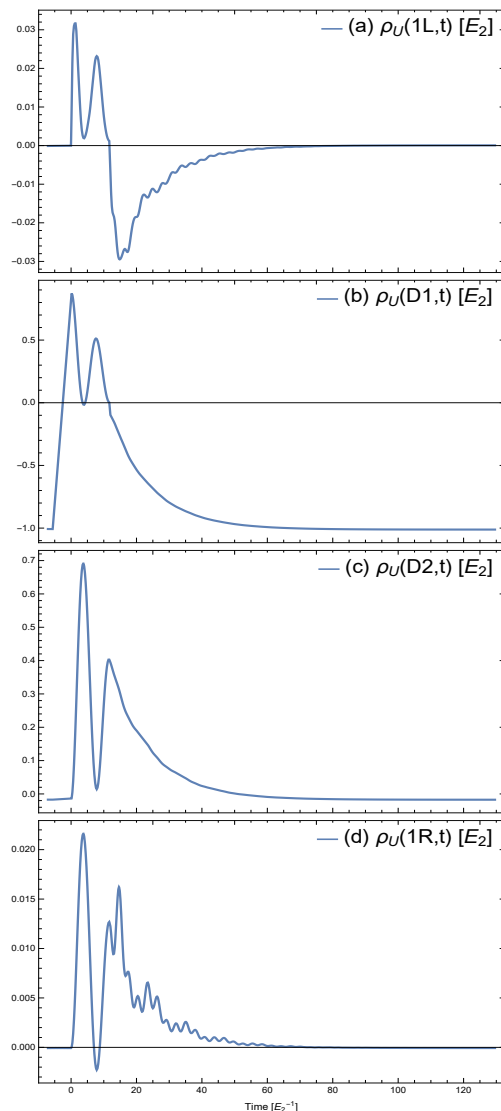


FIG. 7: The internal energy density $\rho_U(x, t)$ plotted for the system depicted in the Right Panel of Fig. 6, but with pulse duration set as a 3π -pulse instead of a π -pulse. The 1.5 periods of Rabi oscillations during the pulse (which is now active up to a time of 11.78 in units of E_2^{-1}) are quite evident in this case. Note that the energy scale for $\rho_U(1L, t)$ and $\rho_U(1R, t)$ is different from that for $\rho_U(D1, t)$ and $\rho_U(D2, t)$ in the figure.

and begins to decrease as the electron tunnels out onto the first site in the right reservoir, eventually relaxing back to its zero initial value. The energy on the first site in the right reservoir $\rho_{U_{sys}}(1R, t)$ (Fig. 6d) can be understood similarly to that on site $1L$ within the bonding picture discussed in the previous paragraph. As the electron tunnels onto $1R$ from the right dot the internal energy there increases followed by an asymptotic decrease to its initial value again almost mimicking the temporal behavior at $D2$.

VI. CONCLUSIONS

In this work, we have clarified a key question in Quantum Thermodynamics: Can the First Law of Thermodynamics be formulated in an unambiguous, experimentally meaningful, and quantum mechanically consistent fashion for open quantum systems driven far from equilibrium? We shed light on this question by employing an insight from Mesoscopics—that far away from the local driving and coupling of the system, the reservoirs stay arbitrarily close to equilibrium—allowing us to unambiguously identify an internal energy operator and consequently a First Law for such systems. The thermodynamic partitioning so introduced identifies the internal

energy of the system as the sum of the system Hamiltonian and the full coupling Hamiltonian describing the System-Reservoir interface $U_{sys}(t) = H_S(t) + H_{SR}$.

We then derived fully general expressions for all the terms appearing in the First Law using the formalism of non-equilibrium Green's functions (NEGF). In our analysis, the system-reservoir coupling can be arbitrarily strong, and our analysis can be readily extended to the general case where the system, coupling, and reservoir are all explicitly time-dependent (see Appendix B). Furthermore, our formal results incorporate electronic and phononic degrees of freedom in both the system and the reservoir as well as electron-electron, electron-phonon, and phonon-phonon interactions in the system. In our analysis, the external electromagnetic field coupling to the electron-phonon system is treated classically, which allows for absorption and stimulated emission of energy quanta, but does not allow spontaneous emission or radiative heat transfer [62].

We also studied the spatio-temporal distribution of the internal energy of a strongly-driven time-dependent open quantum system, shedding light on the internal dynamics of the system as well as on the evolution of the system-reservoir interface. The interface contribution to the internal energy of the system was shown to be localized at the junctions between the system and the reservoirs. For the case of a metallic reservoir in the nearest-neighbor tight-binding model, with only nearest-neighbor bonds to the system, the interface energy was found to be entirely localized on the system-reservoir bonds. The sign of the interface energy can vary from negative to positive, corresponding to bonding or antibonding character of the interface, respectively.

We applied our formal results to a strongly driven quantum machine utilizing Rabi Oscillations between states of a double quantum dot coupled to metallic reservoirs. We presented a full thermodynamic analysis for the machine's operation as both an electrochemical pump and a heat engine, illustrating the utility of our theoretical framework and the power of our computational approach based on NEGF.

It should be remarked that although the First Law clearly holds at the level of quantum statistical averages, provided the energetics are partitioned properly, one cannot expect it to hold at the level individual quantum trajectories, since the operators for internal energy, heat current, and chemical power (among others) do not commute, and hence these are incompatible observables [20].

It is hoped that our very general derivation of the First Law of Thermodynamics in time-dependent open quantum systems, illustrated with applications of our theory to specific examples of model quantum thermal machines, will help to resolve once and for all the controversy over the validity of First Law of Thermodynamics in open quantum systems.

VII. ACKNOWLEDGMENTS

It is a pleasure to acknowledge several helpful discussions with Caleb M. Webb, Marco A. Jimenez-Valencia, and Carter S. Eckel during various stages of this work. We also thank J. M. Van Ruitenbeek for suggesting the valuable generalization of incorporating phonons in our model. This work was partially supported by the U.S. Department of Energy (DOE), Office of Science under Award No. DE-SC0006699.

-
- [1] A. Shastry, S. Inui, and C. A. Stafford, Scanning tunneling thermometry, *Physical Review Applied* **13**, 024065 (2020).
- [2] M. Mecklenburg, W. A. Hubbard, E. R. White, R. Dhall, S. B. Cronin, S. Aloni, and B. C. Regan, Nanoscale temperature mapping in operating microelectronic devices, *Science (New York, N.Y.)* **347**, 629 (2015).
- [3] P. Neumann, I. Jakobi, F. Dolde, C. Burk, R. Reuter, G. Waldherr, J. Honert, T. Wolf, A. Brunner, J. H. Shim, D. Suter, H. Sumiya, J. Isoya, and J. Wrachtrup, High-precision nanoscale temperature sensing using single defects in diamond, *Nano Letters* **13**, 2738 (2013), pMID: 23721106.
- [4] W. Jeong, S. Hur, E. Meyhofer, and P. Reddy, Scanning probe microscopy for thermal transport measurements, *Nanoscale and Microscale Thermophysical Engineering* **19**, 279 (2015).
- [5] F. Menges, P. Mensch, H. Schmid, H. Riel, A. Stemmer, and B. Gotsmann, Temperature mapping of operating nanoscale devices by scanning probe thermometry, *Nature Communications* **7**, 10874 EP (2016), article.
- [6] L. Shi, J. Zhou, P. Kim, A. Bachtold, A. Majumdar, and P. L. McEuen, Thermal probing of energy dissipation in current-carrying carbon nanotubes, *Journal of Applied Physics* **105**, 104306 (2009).
- [7] K. Kim, W. Jeong, W. Lee, and P. Reddy, Ultra-high vacuum scanning thermal microscopy for nanometer resolution quantitative thermometry, *ACS Nano* **6**, 4248 (2012), pMID: 22530657.
- [8] W. Lee, K. Kim, W. Jeong, L. A. Zotti, F. Pauly, J. C. Cuevas, and P. Reddy, Heat dissipation in atomic-scale junctions, *Nature* **498**, 209 (2013).
- [9] S. Gomès, A. Assy, and P.-O. Chapuis, Scanning thermal microscopy: A review, *physica status solidi (a)* **212**, 477 (2015).
- [10] L. Cui, W. Jeong, S. Hur, M. Matt, J. C. Klöckner, F. Pauly, P. Nielaba, J. C. Cuevas, E. Meyhofer, and P. Reddy, Quantized thermal transport in single-atom junctions, *Science (New York, N.Y.)* **355**, 1192 (2017).
- [11] N. Mosso, U. Drechsler, F. Menges, P. Nirmalraj, S. Karg, H. Riel, and B. Gotsmann, Heat transport through atomic contacts, *Nat Nano* **12**, 430 (2017), letter.
- [12] S. Toyabe, T. Sagawa, M. Ueda, E. Muneyuki, and M. Sano, Experimental demonstration of information-to-energy conversion and validation of the general-

- ized Jarzynski equality, *Nature Physics* **6**, 988 (2010), [arXiv:1009.5287 \[cond-mat.stat-mech\]](https://arxiv.org/abs/1009.5287).
- [13] A. Bérut, A. Arakelyan, A. Petrosyan, S. Ciliberto, R. Dillenschneider, and E. Lutz, Experimental verification of Landauer’s principle linking information and thermodynamics, *Nature* **483**, 187 (2012).
- [14] J. V. Koski, V. F. Maisi, J. P. Pekola, and Dmitri V. Averin, Experimental realization of a Szilard engine with a single electron, *Proceedings of the National Academy of Sciences* **111**, 13786 (2014).
- [15] M. H. Devoret, B. Huard, R. Schoelkopf, and L. F. Cugliandolo, eds., *Quantum Machines: Measurement and Control of Engineered Quantum Systems*, first edition ed. (Oxford University Press, Oxford, United Kingdom, 2014).
- [16] M. Campisi, P. Hänggi, and P. Talkner, *Colloquium* : Quantum fluctuation relations: Foundations and applications, *Reviews of Modern Physics* **83**, 771 (2011).
- [17] C. Jarzynski, Equalities and Inequalities: Irreversibility and the Second Law of Thermodynamics at the Nanoscale, *Annual Review of Condensed Matter Physics* **2**, 329 (2011).
- [18] U. Seifert, Stochastic thermodynamics, fluctuation theorems, and molecular machines, *Reports on Progress in Physics* **75**, 126001 (2012), [arXiv:1205.4176](https://arxiv.org/abs/1205.4176).
- [19] S. Deffner and S. Campbell, *Quantum Thermodynamics*, 2053-2571 (Morgan & Claypool Publishers, 2019).
- [20] P. Talkner and P. Hänggi, *Colloquium* : Statistical mechanics and thermodynamics at strong coupling: Quantum and classical, *Reviews of Modern Physics* **92**, 041002 (2020).
- [21] M. F. Ludovico, J. S. Lim, M. Moskalets, L. Arrachea, and D. Sánchez, Dynamical energy transfer in ac-driven quantum systems, *Physical Review B* **89**, 161306 (2014).
- [22] A. Bruch, M. Thomas, S. Viola Kusminskiy, F. von Oppen, and A. Nitzan, Quantum thermodynamics of the driven resonant level model, *Physical Review B* **93**, 115318 (2016).
- [23] P. Strasberg and A. Winter, First and Second Law of Quantum Thermodynamics: A Consistent Derivation Based on a Microscopic Definition of Entropy, *PRX Quantum* **2**, 030202 (2021).
- [24] A. M. Lacerda, A. Purkayastha, M. Kewming, G. T. Landi, and J. Goold, *Quantum thermodynamics with fast driving and strong coupling via the mesoscopic leads approach* (2022), [arXiv:2206.01090](https://arxiv.org/abs/2206.01090).
- [25] N. Bergmann and M. Galperin, A Green’s function perspective on the nonequilibrium thermodynamics of open quantum systems strongly coupled to baths: Nonequilibrium quantum thermodynamics, *The European Physical Journal Special Topics* **230**, 859 (2021).
- [26] H. Haug and A.-P. Jauho, *Quantum Kinetics in Transport and Optics of Semiconductors*, 2nd ed. (Springer, Berlin ; New York, 2007).
- [27] G. Stefanucci and R. van Leeuwen, *Nonequilibrium Many-Body Theory of Quantum Systems: A Modern Introduction* (Cambridge University Press, Cambridge, 2013).
- [28] T. Dittrich, H. P., G.-L. Ingold, B. Kramer, S. G., and W. Zwerger, *Quantum Transport and Dissipation*, hardcover ed. (Wiley-VCH, 1998).
- [29] M. Büttiker, Time-Dependent Transport in Mesoscopic Structures, *Journal of Low Temperature Physics* **118**, 519 (2000).
- [30] J. D. Barr, C. A. Stafford, and J. P. Bergfield, Effective field theory of interacting π electrons, *Physical Review B* **86**, 115403 (2012).
- [31] J. P. Bergfield, J. D. Barr, and C. A. Stafford, The Number of Transmission Channels Through a Single-Molecule Junction, *ACS Nano* **5**, 2707 (2011), doi: 10.1021/nn1030753.
- [32] J. P. Bergfield, J. D. Barr, and C. A. Stafford, Transmission eigenvalue distributions in highly conductive molecular junctions., *Beilstein journal of nanotechnology* **3**, 40 (2012).
- [33] The clarification about the spatial extent of the coupling is of direct relevance to the central result of this work and one that needs highlighting in view of some ambiguity existing about the physical nature of H_{SR} in other works [34], that attempt to tackle the same problem with a different set of tools.
- [34] P. Strasberg, Chapter 3 - Quantum Thermodynamics Without Measurements, in *Quantum Stochastic Thermodynamics: Foundations and Selected Applications*, Oxford Graduate Texts (Oxford University Press, Oxford, New York, 2022).
- [35] N. W. Ashcroft and N. D. Mermin, Chapter 20 - Cohesive Energy, in *Solid State Physics* (Holt, Rinehart and Winston, New York, 1976) pp. 395–414.
- [36] C. Jarzynski, Comparison of far-from-equilibrium work relations, *Comptes Rendus Physique* **8**, 495 (2007).
- [37] G. N. Bochkov and I. E. Kuzovlev, General theory of thermal fluctuations in nonlinear systems, *Zhurnal Eksperimentalnoi i Teoreticheskoi Fiziki* **72**, 238 (1977).
- [38] L. E. Ballentine, Chapter 3 - Kinematics and Dynamics, in *Quantum Mechanics: A Modern Development* (World Scientific Publishing, 2014) 2nd ed.
- [39] J. P. Bergfield and C. A. Stafford, Thermoelectric signatures of coherent transport in single-molecule heterojunctions, *Nano Letters* **9**, 3072 (2009).
- [40] M. Galperin, A. Nitzan, and M. A. Ratner, Heat conduction in molecular transport junctions, *Physical Review B* **75**, 155312 (2007).
- [41] L. Landau and E. Lifshitz, CHAPTER II - THERMODYNAMIC QUANTITIES, in *Statistical Physics (Third Edition)* (Butterworth-Heinemann, Oxford, 1980) third edition ed., pp. 34–78.
- [42] M. Büttiker, Role of quantum coherence in series resistors, *Physical Review B* **33**, 3020 (1986).
- [43] H. U. Baranger and A. D. Stone, Electrical linear-response theory in an arbitrary magnetic field: A new Fermi-surface formation, *Physical Review B* **40**, 8169 (1989).
- [44] J. U. Nöckel, A. D. Stone, and H. U. Baranger, Adiabatic turn-on and the asymptotic limit in linear-response theory for open systems, *Physical Review B* **48**, 17569 (1993).
- [45] P. Talkner, E. Lutz, and P. Hänggi, Fluctuation theorems: Work is not an observable, *Physical Review E* **75**, 050102 (2007).
- [46] P. Talkner and P. Hänggi, Aspects of quantum work, *Physical Review E* **93**, 022131 (2016).
- [47] C. M. Webb and C. A. Stafford, Densities and fluxes of many-body observables, unpublished (2022).
- [48] C. A. Stafford, M. A. Jimenez Valencia, C. M. Webb, and F. Evers, Entropy density and flux in topological and nonequilibrium quantum systems, in *APS March Meeting Abstracts*, APS Meeting Abstracts, Vol. 2022 (2022) p.

- K50.00005.
- [49] L. P. Kadanoff and G. Baym, *Quantum Statistical Mechanics* (New York, W.A. Benjamin, New York, 1962).
- [50] L. V. Keldysh, Diagram technique for nonequilibrium processes, *Zh. Eksp. Teor. Fiz.* **47**, 1515 (1964).
- [51] J. Rammer, *Quantum Field Theory of Non-equilibrium States* (Cambridge: Cambridge University Press, Cambridge, 2007).
- [52] V. Gasparian, T. Christen, and M. Büttiker, Partial densities of states, scattering matrices, and Green's functions, *Physical Review A* **54**, 4022 (1996).
- [53] H.-P. Breuer and F. Petruccione, *The Theory of Open Quantum Systems* (Oxford University Press, Oxford ; New York, 2002).
- [54] N. S. Wingreen, A.-P. Jauho, and Y. Meir, Time-dependent transport through a mesoscopic structure, *Physical Review B* **48**, 8487 (1993).
- [55] A.-P. Jauho, N. S. Wingreen, and Y. Meir, Time-dependent transport in interacting and noninteracting resonant-tunneling systems, *Physical Review B* **50**, 5528 (1994).
- [56] Y. Meir and N. S. Wingreen, Landauer formula for the current through an interacting electron region, *Physical Review Letters* **68**, 2512 (1992).
- [57] C. A. Stafford and N. S. Wingreen, Resonant Photon-Assisted Tunneling through a Double Quantum Dot: An Electron Pump from Spatial Rabi Oscillations, *Physical Review Letters* **76**, 1916 (1996).
- [58] S. Datta, *Electronic Transport in Mesoscopic Systems*, Cambridge Studies in Semiconductor Physics and Microelectronic Engineering (Cambridge University Press, Cambridge, 1995).
- [59] S. Datta, Chapter 8 - Level broadening, in *Quantum Transport: Atom to Transistor* (Cambridge University Press, Cambridge, 2005).
- [60] J. Bergfield, *Many-Body Theory of Electrical, Thermal and Optical Response of Molecular Heterojunctions*, Ph.D. thesis, The University of Arizona. (2010).
- [61] In the computational solution, the broad-band limit was used, which consists in taking the limit $t_0 \rightarrow \infty$ while keeping t^2/t_0 fixed.
- [62] S.-A. Biehs, E. Rousseau, and J.-J. Greffet, Mesoscopic description of radiative heat transfer at the nanoscale, *Physical Review Letters* **105**, 234301 (2010).
- [63] G. D. Mahan, *Many-Particle Physics*, 3rd ed. (New York : Kluwer Academic/Plenum Publishers, New York, 2000).
- [64] J. M. Ziman, *Electrons and Phonons: The Theory of Transport Phenomena in Solids* (Oxford University Press, 2001).

Appendix A: Derivation of the NEGF formulas for all First Law quantities

In this appendix, we give the details of the derivation of the electronic heat current formula in terms of the System Green's functions using the Nonequilibrium Green's function (NEGF) formalism [26, 27, 49–51]. (The calculation of the interface internal energy [Eq. (49)] proceeds in a nearly parallel fashion.)

To derive the heat current formula [Eq. (40)], we begin with the electronic heat current given in terms of expectation values in Eq. (20). We then define the lesser Tunneling Green's functions [the equal time version of these was defined in Sec. IV as $G_{tun, kn}^{<, el}(t, t)$]:

$$G_{nk}^{<, el}(t, t_1) = i\langle c_k^\dagger(t_1)d_n(t) \rangle, \quad (\text{A1})$$

and

$$G_{kn}^{<, el}(t, t_1) = i\langle d_n^\dagger(t_1)c_k(t) \rangle, \quad (\text{A2})$$

noting that at equal times $G_{nk}^{<, el}(t, t) = -[G_{kn}^{<, el}(t, t)]^*$. With this, we can write the heat current as

$$I_{\alpha, el}^Q(t) = \frac{-2}{\hbar} \text{Re} \left[\sum_{k \in \alpha, n} (\epsilon_k - \mu_\alpha) V_{kn}^{el} G_{nk}^{<, el}(t, t) \right]. \quad (\text{A3})$$

The NEGF prescription tells us that $G_{nk}^{<, el}(t, t')$ will be a component of the Contour-Ordered Tunneling Green's function

$$G_{nk}^{\mathcal{T}}(\tau, \tau') = -i\langle \mathcal{T}(d_n(\tau)c_k^\dagger(\tau')) \rangle, \quad (\text{A4})$$

where τ is the contour time. The equation of motion of the Contour-Ordered Tunneling Green's function is

$$-i \frac{\partial}{\partial \tau'} G_{nk}^{\mathcal{T}}(\tau, \tau') = \epsilon_k G_{nk}^{\mathcal{T}}(\tau, \tau') + \sum_m G_{nm}^{\mathcal{T}}(\tau, \tau') (V_{km}^{el})^*, \quad (\text{A5})$$

where $G_{nm}^{\mathcal{T}}(\tau, \tau') = -i\langle \mathcal{T}(d_n(\tau)d_m^\dagger(\tau')) \rangle$ is the Contour-Ordered *System* Green's function and we get

$$G_{nk}^{\mathcal{T}}(\tau, \tau') = \sum_m \int d\tau_1 G_{nm}^{\mathcal{T}}(\tau, \tau_1) (V_{km}^{el})^* g_k^{\mathcal{T}}(\tau_1, \tau'), \quad (\text{A6})$$

by using the equation of motion of the uncoupled Contour-Ordered reservoir Green's function $g_k^T(\tau, \tau') = -i\langle c_k(\tau), c_k^\dagger(\tau') \rangle$. The physical lesser component of the Contour-Ordered Tunneling Green's function [Eq. (A6)] can be found using the so-called Langreth rules [26, 27], giving

$$G_{nk}^{<,el}(t, t') = \sum_m \int dt_1 (V_{km}^{el})^* [G_{nm}^{R,el}(t, t_1) g_k^<(t_1, t') + G_{nm}^{<,el}(t, t_1) g_k^A(t_1, t')]. \quad (\text{A7})$$

The lesser and advanced uncoupled Reservoir Green's functions are given by

$$g_k^<(t, t') = i\langle c_k^\dagger(t') c_k(t) \rangle = if(\epsilon_k^0) \exp(-i\epsilon_k(t - t')) \quad (\text{A8})$$

and

$$g_k^A(t, t') = i\theta(t' - t) \langle \{c_k(t), c_k^\dagger(t')\} \rangle = i\theta(t' - t) \exp(-i\epsilon_k(t - t')), \quad (\text{A9})$$

respectively, where

$$f(\epsilon_k^0) = \frac{1}{e^{\beta_\alpha(\epsilon_k^0 - \mu)} + 1} \quad (\text{A10})$$

is the Fermi-Dirac distribution function. Putting this all together, we can write

$$I_{\alpha,el}^Q(t) = \frac{2}{\hbar} \mathbb{I}m \left[\sum_{k \in \alpha, n, m} (\epsilon_k - \mu_\alpha) \int_{-\infty}^t dt_1 \{ e^{-i\epsilon_k(t_1 - t)} V_{kn}^{el} (V_{km}^{el})^* [G_{nm}^{<,el}(t, t_1) + f_\alpha(\epsilon_k) G_{nm}^{R,el}(t, t_1)] \} \right], \quad (\text{A11})$$

which, upon defining the tunneling width-matrix as in Eq. (39), allows us to turn the momentum sum into an energy integral and can be written, by going over to the matrix notation, as

$$I_{\alpha,el}^Q(t) = \frac{2}{\hbar} \int_{-\infty}^{\infty} \frac{dE}{2\pi} \int_{-\infty}^t dt_1 (E - \mu_\alpha) \mathbb{I}m \mathbb{T}r \{ e^{-iE(t_1 - t)} \Gamma_\alpha^{el}(E) [G^{<,el}(t, t_1) + f_\alpha(E) G^{R,el}(t, t_1)] \}, \quad (\text{A12})$$

which is exactly Eq. (40). The phononic heat current Eq. (42) can be obtained in an analogous manner in terms of phononic Green's functions $G^{<,ph}$ and $G^{R,ph}$, starting from Eq. (22). The interfacial contribution to the internal energy, $\langle H_{SR} \rangle$ [Eq. (49)], can be derived in a similar fashion.

The internal energy density $\rho_{U_{sys}}(x, t)$ [Eq. (34)] can also be evaluated in terms of the system Green's function. Since $\rho_{H_S}(x, t)$ is already given in terms of the system Green's function in Eq. (50), we need to evaluate only $\rho_{H_{SR}}(x, t)$ [Eq. (51)]. Again, by employing the same procedure used for deriving the heat current equation [Eq. (A12)] just discussed, we get

$$\rho_{H_{SR}}(x, t) = \int_{-\infty}^{\infty} \frac{dE}{2\pi} \int_{-\infty}^t dt_1 \mathbb{I}m \{ \langle x | e^{-iE(t_1 - t)} \Gamma_\alpha^{el}(E) [G^{<,el}(t, t_1) + f_\alpha(E) G^{R,el}(t, t_1)] | x \rangle \}. \quad (\text{A13})$$

Within the framework of NEGF, the Retarded Green's function $G^R(t, t')$, which describes the dynamics of the system, can be computed using the Dyson Equation

$$G^R(t, t') = G_0^R(t, t') + \int_{-\infty}^{\infty} dt_1 \int_{-\infty}^{\infty} dt_2 G_0^R(t, t_1) \Sigma^R(t_1, t_2) G^R(t_2, t'), \quad (\text{A14})$$

where $G_0^R(t, t')$ is the Green's function for the non-interacting and uncoupled system and the Self-Energy function which encodes the interactions and tunneling is given by

$$\Sigma^R(t, t') = \Sigma_{int}^R + \Sigma_{tun}^R(t, t'), \quad (\text{A15})$$

where Σ_{int}^R is the retarded interaction self-energy of the system (for example, the Coulomb self-energy) and the retarded tunneling self-energy is given by

$$\Sigma_{tun}^R(t, t') = \sum_\alpha \int_{-\infty}^{\infty} \frac{dE}{2\pi} e^{-iE(t - t')} [\Lambda_\alpha(E) - \frac{i}{2} \Gamma_\alpha(E)], \quad (\text{A16})$$

with $\Lambda_\alpha(E) = \mathcal{P} \int_{-\infty}^{\infty} \frac{dE'}{2\pi} \frac{\Gamma_\alpha(E')}{E-E'}$, where \mathcal{P} denotes the Principal Value [see, for instance, Eq. (2.26) in [27]]. The Lesser Green's function $G^<(t, t')$, which describes the occupation of the system, can be computed using the Keldysh Equation

$$G^<(t, t') = \int_{-\infty}^{\infty} dt_1 \int_{-\infty}^{\infty} dt_2 G^R(t, t_1) \Sigma^<(t_1, t_2) G^A(t_2, t'), \quad (\text{A17})$$

where we have omitted the so-called memory term [see, for instance, Eq. (5.11) in [26]] since it is not relevant for the protocols we consider in this article, and the lesser Self-Energy function is

$$\Sigma^<(t, t') = \Sigma_{int}^< + i \sum_{\alpha} \int_{-\infty}^{\infty} \frac{dE}{2\pi} e^{-iE(t-t')} f_{\alpha}(E) \Gamma_{\alpha}(E). \quad (\text{A18})$$

The two-body Green's function $G^{(2),el}(t, t)$ appearing in Eq. (48) can be evaluated directly using the Bethe-Salpeter equation [27], or the contribution from electron-electron interactions to Eq. (48) can be evaluated using the Coulomb self-energy and the one-body Green's function. The electron-phonon Green's function $G^{(2),el-ph}(t, t)$ and the higher-order phonon Green's functions such as $G^{(3),ph}(t, t)$, also appearing in Eq. (48), can be evaluated using the well-developed theory of electron-phonon and phonon-phonon interactions [63, 64].

Appendix B: Generalization to Time-Dependent reservoirs and coupling

We generalize our results from section IV to the case of a fully time-dependent Hamiltonian $H(t)$ where, in addition to the System, the Coupling and Reservoirs also acquire explicit time-dependence i.e. $H_{SR} \rightarrow H_{SR}(t)$ and $H_R \rightarrow H_R(t)$ so that

$$H(t) = H_S(t) + H_{SR}(t) + H_R(t). \quad (\text{B1})$$

For notational simplicity, we will again treat only electronic degrees of freedom here, but our results hold with full generality for phononic degrees of freedom as well. The time-dependent System Hamiltonian is then given by

$$H_S(t) = \sum_{n,m} \left([H_S^{(1)}(t)]_{nm} d_n^\dagger d_m + [H_S^{(2)}]_{nm} d_n^\dagger d_m^\dagger d_m d_n \right). \quad (\text{B2})$$

The Reservoirs are modeled with

$$H_R(t) = \sum_{k \in \alpha, \alpha} \epsilon_k(t) c_k^\dagger c_k, \quad (\text{B3})$$

where, following [54], the time dependence of the Reservoir energy levels is assumed to take the form $\epsilon_k(t) = \epsilon_k^0 + \Delta_\alpha(t)$, where ϵ_k^0 is the unperturbed reservoir energy and $\Delta_\alpha(t)$ is a rigid time-dependent energy shift. The System-Reservoir Coupling is given by

$$H_{SR}(t) = \sum_{k \in \alpha, \alpha, n} (V_{kn}(t) c_k^\dagger d_n + h.c.). \quad (\text{B4})$$

The aim again is to compute the particle and heat currents flowing into the reservoirs and see what the First Law of thermodynamics looks like for this setup. The particle current was worked out as a generalization of the Meir-Wingreen formula in [54] and is given by

$$I_\alpha^N(t) = \frac{2}{\hbar} \int_{-\infty}^{\infty} \frac{dE}{2\pi} \int_{-\infty}^t dt_1 \text{Im} \text{Tr} \{ e^{-iE(t_1-t)} \Gamma_\alpha(E; t_1, t) [G^<(t, t_1) + f_\alpha(E) G^R(t, t_1)] \}, \quad (\text{B5})$$

where a generalized *time-dependent* tunneling width matrix $\Gamma_\alpha(E; t_1, t)$ is identified as

$$[\Gamma_\alpha(E; t_1, t)]_{nm} = \sum_{k \in \alpha} 2\pi \delta(E - \epsilon_k) V_n(E, t) V_m^*(E, t_1) e^{i \int_t^{t_1} dt_2 \Delta_\alpha(t_2)}, \quad (\text{B6})$$

with $V_n(E, t) = V_{kn}(t)$ when $E = \epsilon_k$.

Just as in Sec. III [Eq. (19)], the heat current flowing into reservoir α can be evaluated by applying the fundamental thermodynamic identity $dE = TdS + \mu dN$ to that reservoir. This identity still applies since the external driving voltage applied to the reservoir $\Delta_\alpha(t)$ is at microwave frequencies or below, so that the timescale of variation is long compared to the signal propagation time from the system into the reservoir, for typical experimental setups. The reservoirs can thus be assumed to be in quasi-equilibrium and the identification of heat as $dQ = TdS$ in the driven reservoirs is still valid:

$$I_\alpha^Q(t) \equiv T_\alpha \frac{d}{dt} S_\alpha = \frac{d}{dt} \langle H_{R,\alpha}(t) \rangle - \mu_\alpha(t) \frac{d}{dt} \langle N_\alpha \rangle, \quad (\text{B7})$$

where $\mu_\alpha(t) = \mu_\alpha^0 + \Delta_\alpha(t)$ (with μ_α^0 denoting the chemical potential of the reservoir in steady state). Following the same steps that lead to Eq.(A3) in Appendix A, we obtain

$$I_\alpha^Q(t) = \frac{-2}{\hbar} \text{Re} \left[\sum_{k \in \alpha, n} (\epsilon_k^0 - \mu_\alpha^0) V_{kn}(t) G_{nk}^<(t, t) \right], \quad (\text{B8})$$

which upon evaluating $G_{nk}^<(t, t')$ exactly as in appendix A, gives

$$I_\alpha^Q(t) = \frac{2}{\hbar} \text{Im} \left[\sum_{k \in \alpha, n, m} (\epsilon_k^0 - \mu_\alpha^0) \int_{-\infty}^t dt_1 \{ e^{-i\epsilon_k^0(t_1-t)} V_{kn}(t) V_{km}^*(t_1) e^{i \int_t^{t_1} dt_2 \Delta_\alpha(t_2)} [G_{nm}^<(t, t_1) + f_\alpha(E) G_{nm}^R(t, t_1)] \} \right], \quad (\text{B9})$$

where we have used the fact that the uncoupled (but driven) reservoir Green's functions are now given by

$$g_k^<(t, t') = i f(\epsilon_k^0) \exp(-i \int_{t'}^t dt_1 \epsilon_k(t_1)) \quad (\text{B10})$$

and

$$g_k^A(t, t') = i \theta(t' - t) \exp(-i \int_{t'}^t dt_1 \epsilon_k(t_1)). \quad (\text{B11})$$

The heat current is thus given, upon going over to the matrix notation, by

$$I_\alpha^Q(t) = \frac{2}{\hbar} \int_{-\infty}^{\infty} \frac{dE}{2\pi} \int_{-\infty}^t dt_1 (E - \mu_\alpha) \text{Im} \text{Tr} \{ e^{-iE(t_1-t)} \Gamma_\alpha(E; t_1, t) [G^<(t, t_1) + f_\alpha(E) G^R(t, t_1)] \}, \quad (\text{B12})$$

where we have relabeled μ_α^0 as μ_α . Again, the particle and heat currents flowing *into* reservoir α can be written compactly as

$$I_\alpha^{(\nu)}(t) = \frac{2}{\hbar} \int_{-\infty}^{\infty} \frac{dE}{2\pi} \int_{-\infty}^t dt_1 (E - \mu_\alpha)^\nu \text{Im} \text{Tr} \{ e^{-iE(t_1-t)} \Gamma_\alpha(E; t_1, t) [G^<(t, t_1) + f_\alpha(E) G^R(t, t_1)] \}, \quad (\text{B13})$$

where $\nu = 0$ gives the particle current and $\nu = 1$ gives the heat current.

The rate of external work done \dot{W}_{ext} is now given by

$$\dot{W}_{ext}(t) = \frac{-i}{\hbar} \text{Tr} [\dot{H}_S(t) G^<(t, t) + \dot{H}_R(t) g^<(t, t) + \dot{H}_{SR}(t) G_{tun}^<(t, t)]. \quad (\text{B14})$$

We can then see that the Internal Energy operator is still identified as in Eq. (28) (with H_{SR} replaced with $H_{SR}(t)$) and the First Law Equation [Eq. (27)] still holds exactly, even when the Reservoirs and Coupling are explicitly time-dependent.